Am J Pathol *Regular Article*

Aromatase Controls Sjögren's Syndrome-like Lesions through MCP-1 in Target Organ and Adipose Tissue-Associated Macrophages

Akihiko Iwasa,[*] [†] Rieko Arakaki,[*] Naoko Honma,[‡] Aya Ushio,[*] Akiko Yamada,[*] Tomoyuki Kondo,[*] Emi Kurosawa,[*] Satoko Kujiraoka,[*] Takaaki Tsunematsu,[*] Yasusei Kudo,[*] Eiji Tanaka,[†] Noriko Yoshimura,[§] Nobuhiro Harada,[§] Yoshio Hayashi,[*] and Naozumi Ishimaru[*]

From the Department of Oral Molecular Pathology[*] and Department of Orthodontics and Dentofacial Orthopedics[†], Institute of Health Biosciences, The University of Tokushima Graduate School, Tokushima, Japan; Research Team for Geriatric Pathology[‡], Tokyo Metropolitan Institute of Gerontology, Tokyo, Japan; the Department of Biochemistry[§], School of Medicine, Fujita Health University, Toyoake, Japan

Address correspondence to Naozumi Ishimaru, Department of Oral Molecular Pathology, Institute of Health Biosciences, The University of Tokushima Graduate School, 3-18-15 Kuramotocho, Tokushima 770-8504, Japan

E-mail: ishimaru.n@tokushima-u.ac.jp

This work was supported in part by the Funding Program for Next Generation World-Leading Researchers in Japan (LS090), a Grant-in-Aid for Scientific Research (no. 25670798, 24659839, and 23390429) from the Ministry of Education, Science, Sport, and Culture of Japan, and Uehara Memorial Foundation.

Running title: A Role of Aromatase in Sjögren's Syndrome

Abstract

Several autoimmune diseases are known to develop in postmenopausal women. However, the mechanism by which estrogen deficiency influences autoimmunity is unknown. Aromatase is a converting enzyme from androgens to estrogens. In the present study, we used female aromatase gene knockout (*Ar*KO) mice as a model of estrogen deficiency to investigate the molecular mechanism that underlies the onset and development of autoimmunity. Histological analyses showed that inflammatory lesions in the lacrimal and salivary glands of *Ar*KO mice increased with age. Adoptive transfer of spleen cells or bone marrow cells from *Ar*KO mice into recombination activating gene 2 knockout mice failed to induce the autoimmune lesions. Expression of mRNA encoding proinflammatory cytokines and monocyte chemotactic protein-1 (MCP-1) increased in white adipose tissue (WAT) of *Ar*KO mice and was significantly higher than that in wild-type mice. Moreover, an increased number of inflammatory M-1 macrophage was observed in WAT of *Ar*KO mice. A significantly increased MCP-1 mRNA expression of the salivary gland tissue in *Ar*KO was found together with adiposity. Furthermore, the autoimmune lesions in a murine model of Sjögren's syndrome (SS) were exacerbated by administration of an aromatase inhibitor. These results suggest that aromatase may play in a key role in the pathogenesis of SS-like lesions by controlling the target organ and adipose tissue-associated macrophage.

Introduction

Autoimmune disease is caused by multiple factors. One of them is the disruption of self-tolerance.[1,2] Several autoimmune diseases such as rheumatoid arthritis or Sjögren's syndrome (SS) occur in postmenopausal women. Sex steroid hormones such as estrogens may influence the onset or development of autoimmune diseases through an unknown mechanism. [3,4]

SS is an autoimmune disease characterized by a 9:1 ratio of women to men, and almost all SS patients are postmenopausal women.[5] SS targets exocrine glands such as the salivary and lacrimal glands, causing patients with SS to experience dryness of the mouth and dry eyes.[6] We demonstrated that estrogen deficiency caused by ovariectomy exacerbates autoimmune lesions in a murine model of SS.[7] Further, we reported that retinoblastoma-associated protein 48 (RbAp48) induces tissue-specific apoptosis in the salivary and lacrimal glands of mice depending on the level of estrogen deficiency.[8] Moreover, we observed that transgenic expression of *RbAp48* in exocrine glands causes the development of autoimmune exocrinopathy, resembling SS.[9] Although postmenopausal estrogen deficiency triggers the breakdown of immune tolerance and induces autoimmune disease, multiple direct or indirect factors that are affected by the change in estrogen level impede efforts to understand the molecular mechanisms involved in autoimmunity.

Estrogens are synthesized from androgens by aromatase, a key step in the biosynthesis of estrogens. Studies on aromatase knockout (*Ar*KO) mice show that aromatase/estrogens plays key roles in controlling sex-specific morphological, neuroendocrinological, and behavioral differences in the brain.[10–12] Further, *Ar*KO mice

develop marked abdominal adiposity, suggesting that aromatase/estrogens controls the adipose phenotype through the regulation of lipid metabolism.[13,14] Moreover, *Ar*KO mice spontaneously develop an autoimmune disease, resembling age-associated SS lesions through B cell hyperplasia and autoantibody production.[15] In addition, increased number of peripheral blood cell and bone marrow cell, and inflammatory renal lesion are observed in *Ar*KO mice.[15] However, the molecular mechanism responsible for the onset of autoimmunity in exocrine glands through aromatase is unknown. In particular, the relationship between aromatase activity and the function of immune cells, besides B cells, in the onset or development of autoimmune disease must be determined to understand the dysfunction of the immune system in postmenopausal women.

In the present study, we investigated the association of the pathogenesis of autoimmune disease with postmenopausal changes induced by estrogen deficiency. Further, we attempted to define the molecular mechanism that accounts for the breakdown of peripheral immune tolerance with the goal of establishing a new therapeutic strategy to treat gender-specific autoimmune diseases.

Materials and Methods

Mice

Female C57BL/6 (B6) mice were purchased from the Japan SLC Laboratory (Shizuoka, Japan). *Ar*KO mice were obtained from RIKEN BioResource Center (Tsukuba, Japan). Female *Ar*KO were used for this study. Female *Rag2*KO mice were obtained from Taconic. Female NFS/N mice carrying mutant *sld* were reared in our specific pathogen-free mouse colony and given food and water ad libitum. Thymectomy was

performed on day three after birth of the NFS/*sld* mice. All mice were bred in the animal facility of the University of Tokushima under specific pathogen-free conditions. The experiments were approved by the animal ethics board of the University of Tokushima.

Administration of Aromatase Inhibitor

The aromatase inhibitor (AI) exemestane (Sigma-Aldrich, St. Louis, MO) was prepared as an aqueous suspension in 0.5% carboxymethylcellulose (CMC) (Dai-Ichi Chemical Industries, Tokyo, Japan). Intraperitoneal injection of B6 mice (8 weeks old) with 200 μl CMC, containing AI (0, 50, and 200 μg/mouse), was administered. For female Tx-NFS/*sld* mice, AI in CMC was injected every day till 4–8 weeks of age.

Histology

All organs were removed from the mice, fixed with 4% phosphate-buffered formaldehyde (pH 7.2), and prepared for histological examination. Formalin-fixed tissue sections were subjected to hematoxylin-eosin (HE) staining, and three pathologists independently evaluated the histology without being informed of the condition of each mouse. Histological grading was performed according to a previously published method.[16] In brief, the inflammatory lesions of lacrimal and salivary glands were evaluated as followed: slight, no change or slight lymphoid cell infiltration; moderate, lymphoid cell infiltration; and severe, marked lymphoid cell infiltration with tissue destruction.

Adoptive cell transfer

Spleen cells (5×10^6) from female WT and *Ar*KO mice (10 weeks of age) were intravenously transferred into female *Rag2*KO mice (8 weeks of age). In addition, bone marrow cells (5×10^6) from WT and *Ar*KO mice were intravenously transferred into irradiated (8 Gy) *Rag2*KO mice. Twelve weeks after transfer, the pathology of all organs was analyzed.

Flow cytometry

Antibodies against CD4, CD8, CD11c, F4/80, CCR2, and CD206 were conjugated as required to FITC, PE, allophycocyanin–peridin chlorophyll protein, PE-Cy5.5, PE-Cy7, or allophycocyanin–Cy7 (eBioscience, San Diego, CA). A FACScanto flow cytometer (BD Biosciences, Franklin Lakes, NJ) was used to determine the cell populations, and the data were analyzed using FlowJo FACS Analysis software (Tree Star, Ashland, OR).

ELISAs

The α-fodrin (JS-1),[16] SS-A/Ro (Immunovision, Springdale, AR), SS-B/La (Immunovision), or ss-DNA (Immunovision)-specific antibodies in sera from mice were measured using ELISAs as previously described.[16] In brief, the antibodies were added to microtiter wells at a concentration of 1 μg/ml of PBS. Nonspecific sites were absorbed with 1% BSA in PBS. After the plates were washed, diluted sera were added. Horseradish peroxidase-conjugated anti-mouse IgG (heavy and light chains; Vector Burlingame, CA) was added as the secondary antibody, and o-phenylenediamine (OPD; Sigma-Aldrich) buffer was added. Antibodies were measured with an microplate reader

(Bio-Rad Laboratories, Richmond, CA).

Quantitative RT-PCR

Total RNA was extracted from WAT, spleen, salivary glands, and liver using Isogen (Wako Pure Chemical Industries, Osaka, Japan) and subsequently reverse-transcribed. The levels of mRNAs encoding F4/80, MCP-1, TLR-4, NF-κB, IL-6, IL-1β, IFN-γ, TNF-α, IL-10, TGF-β, and β-actin were determined using a PTC-200 DNA Engine Cycler (Bio-Rad Laboratories) with SYBR Premix Ex Taq (Takara Bio, Shiga, Japan). The primer sequences used were as follows: F4/80, forward, 5′-CTTTGGCTATGGGCTTCCAGTC-3′, and reverse, 5′-GCAAGGAGGACAGAGTTTATCGTG -3′; MCP-1, forward, 5′-CTGGATCGGAACCAAATGAG -3′, and reverse, 5′-TGAGGTGGTTGTGGAAAAGG -3′; TLR-4: forward, 5′-CAGTGGTCAGTGTGATTGTGG -3′ and reverse, 5′-TTCCTGGATGATGATGTTGGCAGC-3′; NF-κB: forward, 5′-ATGGCAGACGATGATCCCTA -3′ and reverse, 5′-TAGGCAAGGTCAGAATGCAC-3′; IL-1β: forward, 5′-TGATGAGAATGACCTGTTCT-3′, and reverse, 5′-CTTCTTCAAAGATGAAGGAAA-3′; IL-6, forward, 5′-GCTACCAAACTGGATATAATCAGGA-3′, and reverse, 5′-CCAGGTAGCTATGGTACTCCAGAA-3′; IFN-γ, forward, 5′-AGCGGCTGACTGAACTCAGATTGTAG -3′, and reverse, 5′-GTCACAGTTTTCAGCTGTATAGGG -3′;

IL-10, forward, 5′-ATCGATTTCTCCCCTGTGAA-3′, and reverse, 5′-TGTCAAATTCATTCATGGCCT-3′; TGF-β, forward, 5′-GACCGCAACAACGCCATCTAT-3′, and reverse, 5′-GGCGTATCAGTGGGGGTCAG-3′; Arginase-1, forward, 5′-CAGAAGAATGGAAGAGTCAG-3′, and reverse, 5′-CAGATATGCAGGGAGTCACC-3′; Ym-1, forward, 5′-CAGGTCTGGCAATTCTTCTGAA-3′, and reverse, 5′-GTCTTGCTCATGTGTGTAAGTGA-3′; Fizz-1, forward, 5′-TCCCAGTGAATACTGATGAGA-3′, and reverse, 5′-CCACTCTGGATCTCCCAAGA-3′; β-actin, forward, 5′-GTGGGCCGCTCTAGGCACCA-3′, and reverse, 5′-CGGTTGGCCTTAGGGTTCAGGGGG-3′.

Confocal microscopy

Frozen sections of adipose tissues were fixed using a cold acetone and methanol (1:1) mixture. Whole mounts of WAT were minced into small piece, fixed in 4% paraformaldehyde, permeabilized with 1% Triton X-100 (Thermo Scientific, Waltham, MA) for 1 h, and blocked with 5% goat serum. The frozen sections or whole adipose tissues were stained with Alexa® 488-conjugated anti-mouse F4/80 antibodies (eBiosceince). The nuclear DNA was stained with 4′,6-diamidino-2-phenylindole dihydrochloride (DAPI) (Molecular Probe Inc. Eugene, OR). The tissues were counterstained for 1 h with 5 μM BODIPY 558/568

C12[4,4-difluoro-5-(2-thienyl)-4-bora-3a, 4a-diaza-s-indacene-3-dodecanoic acid (Invitrogen, Carlsbad, CA) to visualize adipocytes. The images were acquired using an LSM 5 PASCAL Confocal Laser-scanning (Carl Zeiss, Jena, Germany).

Oil Red O staining

For staining of lipids, the frozen sections of salivary gland from WT and *Ar*KO mice were fixed with 10% phosphate-buffered formaldehyde, incubated for 1 min in 60% 2-propanol, stained for 15 min with Oil Red O solution (Sigma-Aldrich), rinsed in 60% 2-propanol, and washed with water. The specimens were counterstained with Mayer's hematoxylin solution for 5 min.

Immunohistochemical analysis

For immunohistochemical analysis of MCP-1 in salivary gland, paraffin-embedded sections were deparaffinized and subsequently applied to heat-induced antigen retrieval in 10 mM citrate buffer (pH 6.0). The sections were incubated with rabbit MCP-1 polyclonal antibody (BioSS, Dundee Scotland) or control rabbit immunoglobulin and subsequently developed using horseradish-peroxidase-conjugated anti-rabbit immunoglobulin (Vector Laboratories Ltd., Peterborough, UK), and were counterstained with methyl green.

Statistical analysis

Statistical significance was determined using an unpaired the Student's *t* test.

Results

Inflammatory Lesions of Lacrimal and Salivary Glands in *Ar*KO Mice

*Ar*KO mice spontaneously develop SS-like lesions in their lacrimal and salivary glands.[15] In the present study, using another line of *Ar*KO mice,[17] lacrimal and salivary gland tissues were histopathologically analyzed until the mice reached 18 months of age. Severe inflammatory lesions with lymphocyte infiltration and tissue destruction in the lacrimal and salivary glands of *Ar*KO mice were observed during the first 12 months, which resemble those of human SS (Figure 1A). Although slight or mild inflammation of the lacrimal and salivary glands was observed in wild-type (WT) mice older than 12 months, severe inflammatory lesions significantly increased in *Ar*KO mice of the same age (Figure 1B). A large number of $CD4^+$ T cells as well as $B220^+$ cells infiltrated the salivary glands of the *Ar*KO mice (Supplemental Figure 1A). Moreover, significantly higher levels of autoantibodies such as anti-SSA, anti-SSB, and anti-ssDNA, were detected in the sera of *Ar*KO mice compared with those in the sera of WT mice (Supplemental Figure 1B). These findings are consistent with the results of another study that demonstrated that hyperactivation of B cells contributes to the onset of SS-like autoimmune lesions in lacrimal and salivary glands of *Ar*KO mice .[15]

To determine the contribution of peripheral immune cells, including B cells, to the onset of autoimmunity in *Ar*KO mice, 5×10^6 spleen cells from WT or *Ar*KO mice were intravenously transferred into recombination activating gene 2 knockout (*Rag2*KO) mice. Twelve weeks after transfer, all organs were pathologically analyzed. Neither WT nor *Ar*KO spleen cells induced inflammatory lesions in the lacrimal or salivary glands of the recipient mice (Figure 1C). Further, there were no differences in the serum levels of autoantibodies, including anti-SSA, anti-SSB, anti-α-fodrin, and anti-ssDNA (Figure

1D).[9] Moreover, transfer of bone marrow cells from *Ar*KO mice into irradiated *Rag2*KO mice could not induce inflammatory lesion in salivary glands (Supplemental Figure 2A). In addition, the serum level of autoantibodies of the recipient mice transplanted with bone marrow cells from *Ar*KO mice was similar to that from WT mice (Supplemental Figure 2B). These findings suggest that the transfer of immune cells from *Ar*KO mice failed to induce SS-like lesions in the target exocrine glands. Moreover, they suggest that other factors influence the onset or development of inflammatory lesion in *Ar*KO mice.

Relationship between Adipose Tissue and Immune Cells of *Ar*KO Mice

Aromatase is abundantly present in the adipose tissues,[18] and the adipocytes of *Ar*KO mice are significantly larger and more abundant compared with those of WT mice.[14] Furthermore, monocytes or cytokines in adipose tissue contribute to the pathogenesis of autoimmune disease.[19,20] Therefore, we focused on adipose tissues to determine whether they were involved in inducing the SS-like lesions in *Ar*KO mice. The volume of abdominal white adipose tissue (WAT) in female *Ar*KO mice at 12 months of age was greater than that of WT mice (Figure 2A). There was a slight but insignificant increase in body weight of *Ar*KO mice compared with WT mice. However, the weight of WAT of *Ar*KO mice was significantly increased (Figure 2B). Moreover, flow cytometric analysis showed that the proportion of dendritic cells (DCs) and macrophages in the WAT of *Ar*KO mice was higher than that of WT mice (Figure 2C) as well as the absolute numbers of DCs and macrophages (Figure 2D). These findings suggest that increased numbers of DCs and macrophages in WAT may influence the onset or development of

SS-like lesions.

Expression of mRNAs Encoding Macrophage-Associated Proteins in WAT of *Ar*KO Mice

To understand the characteristics of macrophages that accumulated in the adipose tissues of *Ar*KO mice, the expression levels of macrophage-associated genes were quantified using real-time reverse transcription polymerase chain reaction (RT-PCR). We detected significantly increased expression of mRNAs encoding cell surface glycoprotein F4/80 and monocyte chemotactic protein-1 (MCP-1) in the WAT of *Ar*KO mice compared with WT mice (Figure 3A). The expression levels of mRNAs encoding Toll-like receptor-4 (TLR-4) and nuclear factor-κB (NF-κB) in *Ar*KO mice were significantly higher than that in WT mice (Figure 3A).

Macrophage phenotypes are defined as M1 and M2 according to their production of certain cytokines.[21] M1-macrophages produce the proinflammatory cytokines interleukin (IL)-1β, IL-6, interferon (IFN)-γ, and tumor necrosis factor (TNF)-α. In contrast, M2-macrophages produce the anti-inflammatory cytokines IL-10 and tumor growth factor (TGF)-β. The expression levels of mRNAs encoding IL-1β, IL-6, IFN-γ, and TNF-α mRNA in WAT of *Ar*KO mice were significantly increased compared with that in WT mice (Figure 3B). In contrast, expression levels of mRNAs encoding IL-10 and TGF-β mRNA of WAT in *Ar*KO mice were significantly reduced (Figure 3B). In addition, there was no significant difference in mRNA expression of M2-macrophage markers such as Arginase-1, Fizz-1, and Ym-1 in WAT between WT and *Ar*KO mice (Figure 3B). These findings suggest that aromatase regulates the migration and

differentiation of macrophages in adipose tissues as well as their subsequent activation.

Macrophages in Adipose Tissues of *Ar*KO Mice

The distribution of macrophages in WAT was evaluated using immunofluorescence microscopy. Hematoxylin–eosin (HE) staining of adipose tissue sections revealed the accumulation of mononuclear cells around adipocytes in *Ar*KO mice (Figure 4A). Moreover, the accumulated macrophages formed a crown-like structure in the WAT of *Ar*KO mice; this was detected using DAPI (red) staining and an anti-F4/80 monoclonal antibody (green) (Figure 4A). Confocal microscopy revealed that accumlation of $F4/80^+$ macrophages surrounding adipocytes stained with BODIPYR (blue) (Figure 4A). CCR2, a marker of M1-macrophages, was expressed at significantly higher levels by $F4/80^+$ cells in the WAT of *Ar*KO mice compared than in WT mice. In contrast, CD206, a marker of M2-macrophages, was expressed at significantly lower levels in the WAT of *Ar*KO mice than in WT mice (Figure 4B). The results suggest that the increased abundance of WAT in *Ar*KO mice enhanced the migration and maturation of activated M1-macrophages.

Effect of an Aromatase Inhibitor on WAT and Salivary Glands

MCP-1 produced by adipocytes or macrophages plays a key role in chemotaxis of monocytes into adipose tissues.[22] However, it is unclear whether aromatase/estrogens regulate the expression of MCP-1 in WAT. To address this question, we intraperitoneally administered 0, 50, and 200 μg of aromatase inhibitor (AI) into female C57BL/*6* mice daily for one week. Using real-time RT-PCR, we subsequently determined the

expression levels of *Mcp-1* mRNA in various organs. The levels of the mRNA encoding MCP-1 in WAT increased as a function of AI dose (Figure 5). The expression of *Mcp*-1 mRNA in the salivary gland, a target organ of SS, was enhanced by AI treatment, but not in the liver and spleen (Figure 5). These findings demonstrate that the expression of MCP-1 in the salivary glands as well as in WAT is regulated by aromatase/estrogens.

Expression of MCP-1 in Salivary Glands and Cervical WAT

Abundant adipose tissue surrounds the salivary gland, and a change in fat levels is often observed in atrophic salivary glands because of chronic inflammation or aging. When the fatty change of the salivary gland in *Ar*KO mice was compared with that in WT mice using Oil red O staining, more salivary gland cells exhibited a fatty change in *Ar*KO mice (Figure 6A). Moreover, the expression level of *Mcp-1* mRNA of the salivary gland tissue of *Ar*KO mice was significantly increased compared with that of WT mice (Figure 6B). A significantly increased number of $F4/80^{+}$ macrophages in the cervical WAT around the salivary glands of *Ar*KO mice were detected using immunofluorescence staining (Figure 6C). Further, the expression of MCP-1 in the salivary gland of ArKO mice was significantly increased compared with that of WT mice (Figure 6D). In addition, macrophage markers of salivary gland tissues were analyzed by real-time RT-PCR. TLR-4 mRNA of salivary gland from *Ar*KO mice was significantly increased compared with that of WT mice (Supplemental Figure 3). There was no difference in mRNA expression such as IFN-γ, TNF-α, IL-10, and TGF-β in the salivary gland tissues between WT and *Ar*KO mice (Supplemental Figure 3). The findings suggest that MCP-1 may play a key role in the development of SS-like lesions

in the salivary glands.

Effect of AI Administration on Autoimmune Lesions in Mouse Model of Primary SS

To confirm the role of aromatase in the SS-like lesions in the salivary and lacrimal glands, AI was administered into a model for SS which is thymectomized (Tx) NFS/*sld* mouse strain at three days after birth.[23,24] AI (200 μg/mouse) was intraperitoneally administered into Tx NFS/*sld* mice daily from 4 to 8 weeks of age. The severity of autoimmune lesions in the lacrimal and salivary glands of Tx NFS/*sld* mice (8 weeks) was enhanced (Figure 7A). The inflammatory lesions of SS-model mice were markedly more severe compared with those of the control mice (Figure 7B). The proportion of $CD11C^+$DCs and $F4/80^+$ macrophages in the spleens of SS-model mice treated with AI was significantly higher compared with controls (Figure 7C, D). Further, the serum levels of anti-α-fodrin and anti-ssDNA antibodies of AI-treated SS-model mice were significantly higher compared with controls (Figure 7E). These findings suggest that imbalance of aromatase/estrogens may contribute to the onset or development of SS-like lesions through accumulated macrophages or DCs.

Discussion

Evidence indicates that the pathogenesis of autoimmune diseases, such as SS, is influenced by multiple factors.[25] Most autoimmune diseases occur more frequently in women than men.[3,4] In particular, various autoimmune diseases occur in postmenopausal women, who are over middle age around postmenopausal stage. Experimental and clinical evidence suggests that autoimmunity is influenced by several

differences in the immune responses between males and females.[26,27] For example, Th1 and Th2 responses are induced by androgens or estrogens, respectively.[28,29] Among sex hormones, estrogens are the most potent modulator of the immune system, suggesting that a significant change in estrogen levels, such as those that occur during menopause, triggers autoimmunity.[30] Aromatase catalyzes critical steps in the synthesis of estrogens.[31] A number of studies demonstrate that *Ar*KO mice provide an informative animal model for estrogen insufficiency in humans that facilitate our understanding of how estrogens influence the immune system.[12,13,15] Therefore, in the present study, we used *Ar*KO mice to determine whether there is a link between adipose tissue and the immune system with the hope of establishing the molecular basis of the development of autoimmunity.

Shim et al. reported that *Ar*KO mice spontaneously develop SS-like autoimmune lesions through B cell hyperplasia and the production of autoantibodies.[15] The report have demonstrated that estrogen administration into *Ar*KO mice results in preventing SS-like lesions, suggesting that estrogen may play a key role in the pathogenesis of autoimmune lesions of *Ar*KO mice.[15] We also observed SS-like inflammatory lesions in lacrimal and salivary glands and increased autoantibody production by *Ar*KO mice. Moreover, adoptive transfer of both spleen cells and bone marrow cells from *Ar*KO mice into *Rag2*KO mice failed to induce inflammatory lesions, suggesting that in *Ar*KO mice factors other than immune cells contribute to the pathogenesis of SS-like disease. On the other hand, serum concentration of estradiol of *Ar*KO mice is baseline similar to that of WT mice in normal status.[32] Although the estradiol or progesterone level of female WT mice is promoted in the estrus cycle, no change of the level is observed in

female *Ar*KO mice.[32] It is believed that hypotalamis-pituitary axis is disrupted in *Ar*KO mice. Therefore, change of estrogen with diestrous/estrous phase of the cycle is not seen in *Ar*KO mice. In addition, it was reported that prolactin and testosterone levels of the sera in female *Ar*KO mice are significantly elevated compared with those of WT mice.[33] There may be any difference in the physiological function for immune response between estrogen and androgen. Previous reports demonstrated that administration of androgen protects autoimmune lesions in murine SS models.[34,35] However, the function and metabolism of sex hormones are so complicated that the precise molecular mechanism of sex dimorphism in the onset of autoimmunity remains unclear.

It is well known that autoimmunity is multifactorial disease. Although lack of estrogen is important for the onset or development of autoimmunity, the other factors influence the pathogenesis of the autoimmune disease. For instance, when neonatally thymectomized NFS/*sld* mice, one of murine SS models, are ovariectomized during childbearing age, the autoimmune lesions are severely exaggerated.[7] In the present paper, the incidence of autoimmune lesions in *Ar*KO mice is largely increased after 6 months of age, suggesting that aging or unknown factor may influence the onset or development of autoimmunity in the model. On the other hand, there is no report as for inflammatory lesions in *estrogen receptor-α* or *-β* knockout. It is believed that autoimmune disease is triggered by multiple factors. Although deficiency in estrogen/estrogen receptor signaling influences immune responses, only deficiency in the signaling cannot break the immune tolerance to induce autoimmunity. Aromatase may be related with various factors for the pathogenesis of SS-like lesions. However, further research based on sex steroid hormone will be required for understanding the

molecular pathogenesis of autoimmunity.

Aromatase is considerably expressed in adipose tissues, and *Ar*KO mice develop marked abdominal adiposity, which is accompanied by increases in the weight of the gonadal and infrarenal fat pads.[13,14] Adipose tissues in obesity disrupt the immune system and influence the pathogenesis of autoimmune disease.[36,37] Therefore, we determined whether the presence of immune cells in adipose tissues plays a role in autoimmunity in *Ar*KO mice. More important, similar to its effects on adipose tissue, we show that aromatase/estrogens control adiposity and the production of MCP-1 in the salivary gland, a target organ of SS. We speculate that salivary gland cells with adiposity controlled by aromatase may produce MCP-1 to attract macrophages to the target organ. Accumulated M1-macrophages might secrete inflammatory cytokines to enhance SS-like lesions and function as antigen-presenting cells in the target organ to develop SS-like lesions. These findings suggest that the specificity of the salivary gland as a target organ in SS may be explained by the estrogen deficiency-induced phenotypic change of salivary glands.

Excess adiposity increases the risk of developing metabolic syndrome,[38] and obesity is a state of chronic systemic inflammation. Macrophages are considered a crucial component of adipose tissues involved in physiologic and pathologic remodeling.[35] Monocytes are recruited to adipose tissues in obesity to become M1-macrophages and produce MCP-1, IL-1β, IL-6, IFN-γ, and TNF-α to promote systemic proinflammatory signaling.[39,40] In contrast, M2-macrophages produce IL-10 and TGF-β to suppress inflammation.[39,40] Because IL-1β and TGF-β are enzymatically cleaved, the production of the tissues was measured by ELISA. Although IL-1β of

WAT from *Ar*KO mice was significantly increased compared with that from WT mice (WT; 120.3 ± 39.2 pg/WAT, *Ar*KO 191.3 ±52.3 pg/WAT, $p<0.05$), TGF-β was undetectable. It seems to be difficult to quantify the concentration of TGF-β in WAT. M1-macrophages contribute to increased insulin resistance in obesity, and M2-macrophages enhance insulin sensitivity through a PPARγ-dependent mechanism.[22] The development of obesity in *Ar*KO mice occurs at three months of age and is accompanied by a marked increase in the weights of WAT, suggesting that estrogen synthesis regulates lipid metabolism.[14] However, the report did not indicate whether the increased weight of WAT influences the immune system. In the present study, we report that the number of M1-macrophages in the WAT of *Ar*KO mice increased compared with WT mice in addition to the increased WAT. Moreover, our findings suggest that the synthesis of MCP-1 by WAT plays a key role in attracting M1-macrophages to WAT, which induces the preferential production of proinflammatory cytokines.

The role of the aromatase–estrogen axis in the onset or development of autoimmune disease is poorly understood. DCs and macrophages, which are present in WAT and salivary glands, may play a key role in disrupting peripheral immune tolerance and trigger the onset or enhance the development of SS-like lesions. Increased adiposity in the salivary gland resembling that of the WAT in *Ar*KO mice suggests that changes occur in the salivary glands in postmenopausal women with SS. Furthermore, fatty change is observed in the salivary glands of women with SS.[41] Further, a clinical study observed that the expression of MCP-1 is significantly upregulated in salivary gland tissues from patients with SS compared with those from healthy controls.[42] Our present findings suggest that in *Ar*KO mice, adiposity in the salivary gland was due to

estrogen deficiency and further suggest the chain of events as follows: 1. MCP-1 produced by the salivary gland and fat tissue attracted macrophages. 2. The production of several proinflammatory cytokines by these macrophages disrupted local immune tolerance in the salivary gland to trigger the onset of SS. Therefore, estrogen deficiency caused by menopause may link the pathogenesis of SS to an imbalance of cytokine production by macrophages in adipose and target tissues. In addition, our previous paper demonstrated estrogen deficiency triggers or promotes apoptosis of salivary gland cells.[8] Our preliminary experiment showed that increased apoptotic cells were found in aged *Ar*KO mice compared with WT mice. Therefore, it is possible that a part of salivary gland cells with adiposity would undergo apoptosis. Aromatase deficiency results in the low estrogen level or estrogen deficiency. Physiological change of estrogen in female is not observed in *Ar*KO mice. We think that the normal change of estrogen in female through aromatase maintains physiological homeostasis in immune system, fat metabolism, and so on. As described in our paper, aging is also related with the pathogenesis of autoimmunity in *Ar*KO mice. Although the precise molecular mechanism has not been unclear, aromatase may play the key role in the onset or development of SS-like lesions through disturbance of immune cells, adipose tissue, and target organ.

In conclusion, aromatase deficiency resulted in the onset and development of SS-like autoimmune lesions through a switch to cytokine production by M1-macrophages in systemic adipose tissues and target organs. Our findings suggest that decrease of estrogens induced by menopause plays a key role in the pathogenesis of autoimmunity.

Acknowledgments

We thank Ai Katayama, Satoko Katada, and Michiko Kino for the technical assistance.

References

1. Waldmann H: Tolerance: an overview and perspectives. Nat Rev Nephrol 2010, 6:569-576
2. von Boehmer H, Melchers F: Checkpoints in lymphocyte development and autoimmune disease. Nat Immunol 2010, 11:14-20
3. Gleicher N: Postpartum depression, an autoimmune disease? Autoimmun Rev 2007, 6:572-576
4. Cutolo M, Sulli A, Straub RH: Estrogen metabolism and autoimmunity. Autoimmun Rev 2012, 11:A460-464
5. Konttinen YT, Fuellen G, Bing Y, Porola P, Stegaev V, Trokovic N, Falk SS, Liu Y, Szodoray P, Takakubo Y: Sex steroids in Sjögren's syndrome. J Autoimmun 2012, 39:49-56
6. Fox RI: Sjögren's syndrome. Lancet 2005, 366:321-331
7. Ishimaru N, Saegusa K, Yanagi K, Haneji N, Saito I, Hayashi Y: Estrogen deficiency accelerates autoimmune exocrinopathy in murine Sjogren's syndrome through fas-mediated apoptosis. Am J Pathol 1999, 155:173-181

8. Ishimaru N, Arakaki R, Omotehara F, Yamada K, Mishima K, Saito I, Hayashi Y: Novel role for RbAp48 in tissue-specific, estrogen deficiency-dependent apoptosis in the exocrine glands. Mol Cell Biol 2006, 26:2924-2935
9. Ishimaru N, Arakaki R, Yoshida S, Yamada A, Noji S, Hayashi Y: Expression of the retinoblastoma protein RbAp48 in exocrine glands leads to Sjögren's syndrome-like autoimmune exocrinopathy. J Exp Med 2008, 205:2915-2927
10. Hill RA, Boon WC: Estrogens, brain, and behavior: lessons from knockout mouse models. Semin Reprod Med 2009, 27:218-228
11. Hill RA, Chua HK, Jones ME, Simpson ER, Boon WC: Estrogen deficiency results in apoptosis in the frontal cortex of adult female aromatase knockout mice. Mol Cell Neurosci 2009, 41:1-7
12. Bakker J, Pierman S, Gonzalez-Martinez D: Effects of aromatase mutation (ArKO) on the sexual differentiation of kisspeptin neuronal numbers and their activation by same versus opposite sex urinary pheromones. Horm Behav 2010, 57:390-395
13. Jones ME, Thorburn AW, Britt KL, Hewitt KN, Wreford NG, Proietto J, Oz OK, Leury BJ, Robertson KM, Yao S, Simpson ER: Aromatase-deficient (ArKO) mice have a phenotype of increased adiposity. Proc Natl Acad Sci U S A 2000, 97:12735-12740
14. Misso ML, Murata Y, Boon WC, Jones ME, Britt KL, Simpson ER: Cellular and molecular characterization of the adipose phenotype of the aromatase-deficient mouse. Endocrinology 2003, 144:1474-1480
15. Shim GJ, Warner M, Kim HJ, Andersson S, Liu L, Ekman J, Imamov O, Jones ME, Simpson ER, Gustafsson JA: Aromatase-deficient mice spontaneously develop a

lymphoproliferative autoimmune disease resembling Sjögren's syndrome. Proc Natl Acad Sci U S A 2004, 101:12628-12633

16. Kohashi M, Ishimaru N, Arakaki R, Hayashi Y: Effective treatment with oral administration of rebamipide in a mouse model of Sjögren's syndrome. Arthritis Rheum 2008, 58:389-400
17. Honda S, Harada N, Ito S, Takagi Y, Maeda S: Disruption of sexual behavior in male aromatase-deficient mice lacking exons 1 and 2 of the cyp19 gene. Biochem Biophys Res Commun 1998, 252:445-449
18. Bulun SE, Chen D, Moy I, Brooks DC, Zhao H: Aromatase, breast cancer and obesity: a complex interaction. Trends Endocrinol Metab 2012, 23:83-89
19. Toussirot E, Binda D, Gueugnon C, Dumoulin G: Adiponectin in autoimmune diseases. Curr Med Chem 2012, 19:5474-5480
20. Procaccini C, Carbone F, Galgani M, La Rocca C, De Rosa V, Cassano S, Matarese G: Obesity and susceptibility to autoimmune diseases. Expert Rev Clin Immunol 2011, 7:287-294
21. Morris DL, Singer K, Lumeng CN: Adipose tissue macrophages: phenotypic plasticity and diversity in lean and obese states. Curr Opin Clin Nutr Metab Care 2011, 14:341-346
22. Ota T: Chemokine systems link obesity to insulin resistance. Diabetes Metab J 2013, 37:165-172
23. Haneji N, Hamano H, Yanagi K, Hayashi Y: A new animal model for primary Sjögren's syndrome in NFS/sld mutant mice. J Immunol 1994, 153:2769-2777
24. Haneji N, Nakamura T, Takio K, Yanagi K, Higashiyama H, Saito I, Noji S, Sugino

H, Hayashi Y: Identification of alpha-fodrin as a candidate autoantigen in primary Sjögren's syndrome. Science 1997, 276:604-607

25. Voulgarelis M, Tzioufas AG: Pathogenetic mechanisms in the initiation and perpetuation of Sjögren's syndrome. Nat Rev Rheumatol 2010, 6:529-537
26. Cutolo M, Sulli A, Capellino S, Villaggio B, Montagna P, Seriolo B, Straub RH: Sex hormones influence on the immune system: basic and clinical aspects in autoimmunity. Lupus 2004, 13:635-638
27. Nussinovitch U, Shoenfeld Y: The role of gender and organ specific autoimmunity. Autoimmun Rev 2012, 11:A377-385
28. McCarthy M: The "gender gap" in autoimmune disease. Lancet 2000, 356:1088
29. Beagley KW, Gockel CM: Regulation of innate and adaptive immunity by the female sex hormones oestradiol and progesterone. FEMS Immunol Med Microbiol 2003, 38:13-22
30. Nadkarni S, McArthur S: Oestrogen and immunomodulation: new mechanisms that impact on peripheral and central immunity. Curr Opin Pharmacol 2013, 13:576-581
31. Stocco C: Tissue physiology and pathology of aromatase. Steroids 2012, 77:27-35
32. Fisher CR, Graves KH, Parlow AF, and Simpson ER: Characterization of mice deficient in aromatase (ArKO) because of targeted disruption of the cyp19 gene. Proc Natl Acad Sci USA 1998, 95:2965-6970
33. Mcpherson SJ, Wang H, Jones ME, Pedersen J, Iismaa TP, Wreford N, Simpson ER: Elevated androgen and prolactin in aromatase-deficient mice cause enlargement, but not malignancy, of the prostate gland. Endocrinology 2001

142:2458-2467

34. Azzarolo AM, Wood RL, Mircheff AK, Richters A, Olsen E, Berkowitz M, Bachmann M, Huang ZM, Zolfagari R, and Warren DW: Androgen influence on lacrimal gland apoptosis, necrosis, and lymphocyte infiltration. Invest Opthal Vis Sci 1999, 40:592-602
35. Mostafa S, Seamon V, abd Azzarolo AM: Influence of sex hormones and genetic predisposition in Sjögren's syndrome: A new clue to the immunopathogenesis of dry eye disease. Exp Eye Res 2012, 96:88-97
36. Derdemezis CS, Voulgari PV, Drosos AA, Kiortsis DN. Obesity, adipose tissue and rheumatoid arthritis: coincidence or more complex relationship? Clin Exp Rheumatol 2011, 29:712-727
37. Stofkova A: Leptin and adiponectin: from energy and metabolic dysbalance to inflammation and autoimmunity. Endocr Regul 2009, 43:157-168
38. Bartelt A, Heeren J: Adipose tissue browning and metabolic health. Nat Rev Endocrinol 2013, 10:24-36
39. Chawla A, Nguyen KD, Goh YP: Macrophage-mediated inflammation in metabolic disease. Nat Rev Immunol 2011, 11:738-749
40. Han JM, Levings MK: Immune regulation in obesity-associated adipose inflammation. J Immunol 2013, 191:527-532
41. Izumi M, Eguchi K, Nakamura H, Nagataki S, Nakamura T: Premature fat deposition in the salivary glands associated with Sjögren syndrome: MR and CT evidence. AJNR Am J Neuroradiol 1997, 18:951-958
42. Iwamoto N, Kawakami A, Arima K, Nakamura H, Kawashiri SY, Tamai M, Kita J,

Okada A, Koga T, Kamachi M, Yamasaki S, Ichinose K, Ida H, Origuchi T, Eguchi K: Regulation of disease susceptibility and mononuclear cell infiltration into the labial salivary glands of Sjögren's syndrome by monocyte chemotactic protein-1. Rheumatology (Oxford) 2010, 49:1472-1478

Figure Legends

Figure 1 SS-like lesions in the lacrimal and salivary glands of *Ar*KO mice. **A:** Severe inflammatory lesions in the lacrimal glands (LG) and salivary glands (SG) of *Ar*KO mice. Shown are representative images of hematoxylin and eosin (HE)-stained sections of WT and *Ar*KO mice 12 months of age. Scale bar: 200 μm. **B:** Pathological score of inflammatory lesions in LG (upper panel) and SG (lower panel) was evaluated using H&E-stained sections of female WT and *Ar*KO mice from three to 18 months of age (WT, n = 19; ArKO, n = 19). **C:** 5×10^6 spleen cells from WT and *Ar*KO were intravenously transferred into female *Rag2*KO mice at 8 weeks of age. Pathological analysis of the LG and SG of the recipient *Rag2*KO mice was performed three months after transfer. Images are representative of each recipient group (n = 5). **D:** Autoantibody production (anti-SSA, anti-SSB, anti-ssDNA, and anti-α-fodrin antibodies) in the sera of recipient *Rag2*KO mice was analyzed using ELISAs. Data are shown as the average ± standard deviation (SD) of five mice of each group.

Figure 2 Adipose tissues of *Ar*KO mice. **A:** Representative images of WAT of WT and ArKO mice 12 months of age are shown. The lower panel shows formalin-fixed tissues.

Scale bar: 1 cm. **B:** Body weight and WAT weight of WT and *Ar*KO mice were measured at 12 months of age. Data represent the average ± SD of five mice from each group. **p < 0.005. **C:** The proportion of $CD11c^{+}F4/80^{-}$DCs or $F4/80^{+}$ macrophages in WAT of WT and *Ar*KO mice was analyzed using flow cytometry. Results are representative of five mice from each group. **D:** The number of DCs and macrophages in WAT of WT and *Ar*KO mice 12 months of age was evaluated. Cell number is shown as the average ± SD of five mice of each group. *p < 0.05, **p < 0.005.

Figure 3 Real-time reverse transcription polymerase chain reaction of the expression of monocyte-related genes in *Ar*KO and WT mice. (**A**) Levels of mRNAs encoding F4/80, MCP-1, TLR-4, and NF-κB in WAT of WT and *Ar*KO mice 12 months of age. (**B**) The levels of mRNAs encoding IL-1β, IL-6, IFN-γ, TNF-α, IL-10, TGF-β, Arginase-1, Fizz-1, and Ym-1 in WAT of WT and *Ar*KO mice. Data represent the average ± SD of five mice from each group. *p < 0.05, **p < 0.005.

Figure 4 Macrophages infiltrating the WAT of *Ar*KO mice. **A:** H&E-staining of WAT is shown in the upper panel. $F4/80^{+}$ macrophages in WAT of WT and *Ar*KO mice were detected using immunofluorescence staining. Adipocytes were stained with BODIPYR, and $F4/80^{+}$ macrophages in the WAT were detected using a confocal microscope. Nuclei were stained with DAPI. Images represent three mice of each group. DAPI color is shown in red. Images represent three mice from each group. Scale bar: 50 μm. **B:** Flow cytometric analysis of CCR2 and CD206 expression on $F4/80^{+}$ macrophages in the WAT of WT and *Ar*KO mice. Results represent three mice from each group. The gray

line indicates the data for the isotype control. The number of F4/80 positive cells/ mm^2 was counted. Data represent the average ± SD of five mice from each group. *$p < 0.05$, **$p < 0.005$.

Figure 5 Effect of AI on the expression of *Mcp-1* mRNA in various tissues. Daily peritoneal injections of AI (0, 50, and 200 μg/mouse) were administered to female B6 mice 10 weeks of age for a week. The expression of *Mcp-1* mRNA in WAT, salivary glands, liver, and spleen was analyzed using real-time RT-PCR. Data represent the average ± SD of 5 mice of each group. *$p < 0.05$, **$p < 0.005$.

Figure 6 Relationship between fatty change and the expression of *Mcp-1* in the salivary glands of *Ar*KO mice. **A:** Frozen sections of salivary glands in WT and *Ar*KO mice at 10 months of age were stained with Oil Red O. Original magnification: 100× (upper panel, scale bar: 100 μm), 400× (lower panel, scale bar: 20 μm). Images represent three mice from each group. **B**: The expression of *Mcp-1* mRNA in salivary glands of WT and *Ar*KO mice was analyzed using real-time RT-PCR. Data represent the average ± SD of three mice from each group. **$p < 0.005$. **C:** $F4/80^+$ macrophages in the adipose tissue around salivary glands of WT and *Ar*KO mice were detected using immunofluorescence staining. Nuclei were stained with DAPI. Scale bar: 50 μm. The number of F4/80 positive cells/ mm^2 was counted. Data represent the average ± SD of five mice from each group. *$p < 0.05$. **D:** MCP-1^+ cells in the salivary glands of WT and *Ar*KO mice were detected using immunohistochemical analysis. Nuclei were stained with methyl green. Scale bar: 20 μm.

Figure 7 Effect of AI on the autoimmune lesions in SS-model mice. **A:** AI (200 μg) dissolved in CMC was peritoneally injected daily into female Tx-NFS/*sld* mice 4–8 weeks of age. Control Tx-NFS/*sld* mice were injected with CMC. Pathology of lacrimal and salivary glands was determined using HE staining. Photos are representative of five mice from each group. Original magnification: 200×. Scale bar: 100 μm. **B:** Pathological grading was evaluated using HE-stained sections. Data represent the average ± SD of five mice from each group. *$p < 0.05$. **C:** The proportion of monocytes that expressed CD11c and F4/80 was analyzed using flow cytometry. Results are representative of five mice from each group. **D:** $CD11c^+$DCs and $F4/80^+$ macrophages were quantified using flow cytometric analysis. Data represent the average ± standard deviation (SD) of five mice from each group. *$p < 0.05$. **E:** Serum levels of anti-SSA, anti-SSB, anti-α-fodrin and anti-ssDNA antibodies were determined using ELISAs. Data represent the average ± SD of five mice from each group. *$p < 0.05$.

Figure 1

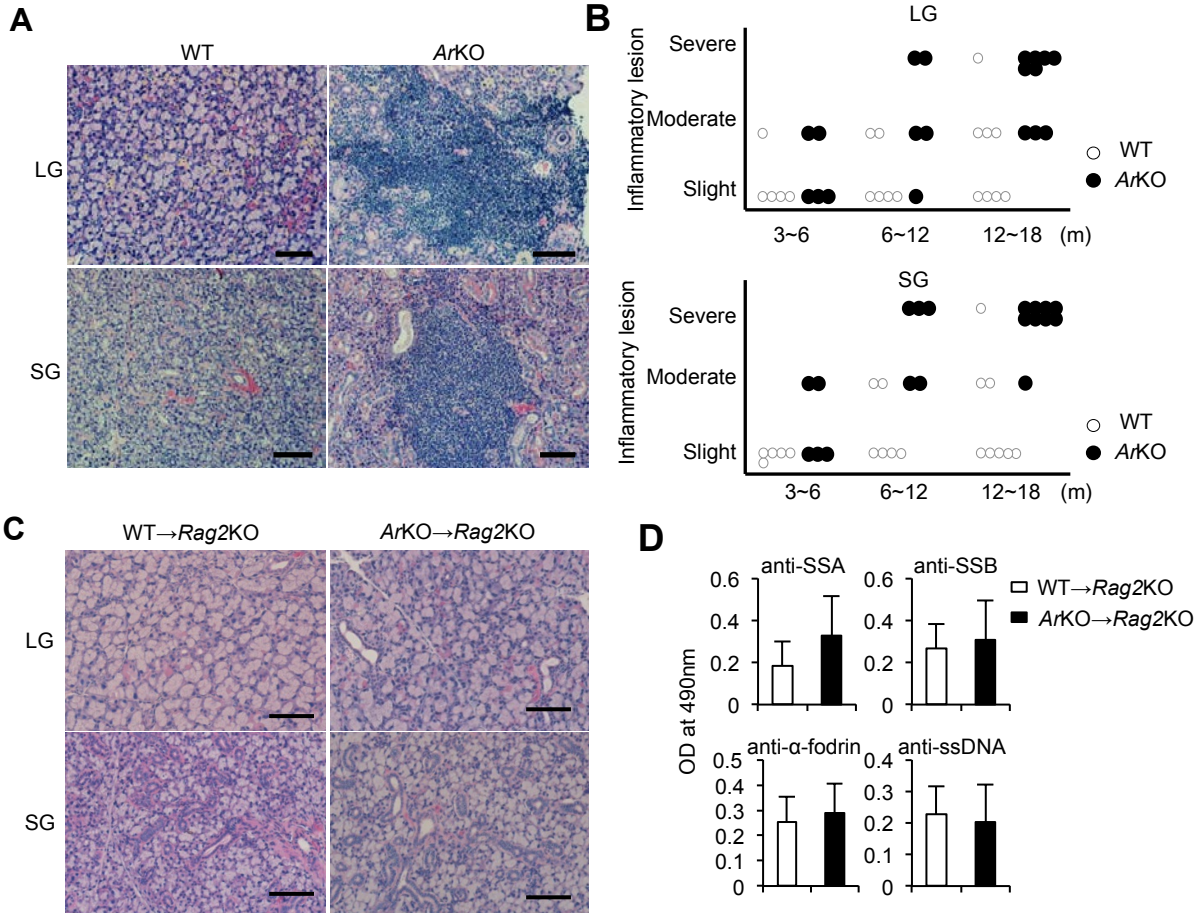
A
WT
ArKO
LG
SG
B
LG
Severe
Moderate
Slight
Inflammatory lesion
3~6
6~12
12~18
(m)
WT
ArKO
SG
C
WT→Rag2KO
ArKO→Rag2KO
D
anti-SSA
anti-SSB
anti-α-fodrin
anti-ssDNA
OD at 490nm

Figure 2

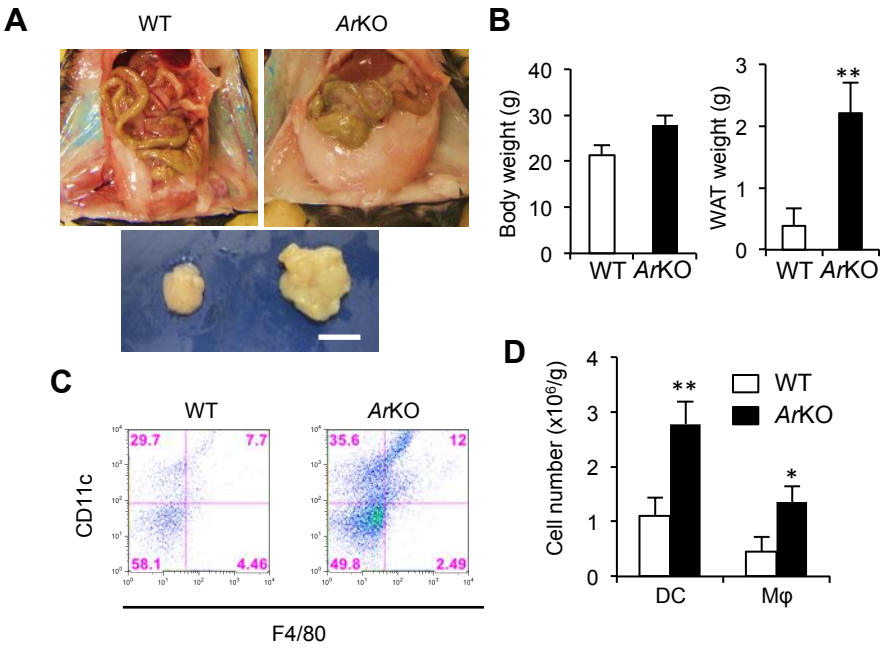
A
WT
ArKO
B
Body weight (g)
40
30
20
10
0
WT
ArKO
WAT weight (g)
3
2
1
0
**
WT
ArKO
C
WT
ArKO
CD11c
29.7
7.7
58.1
4.46
35.6
12
49.8
2.49
F4/80
D
Cell number (x10^6/g)
4
3
2
1
0
**
*
WT
ArKO
DC
Mφ

Figure 3

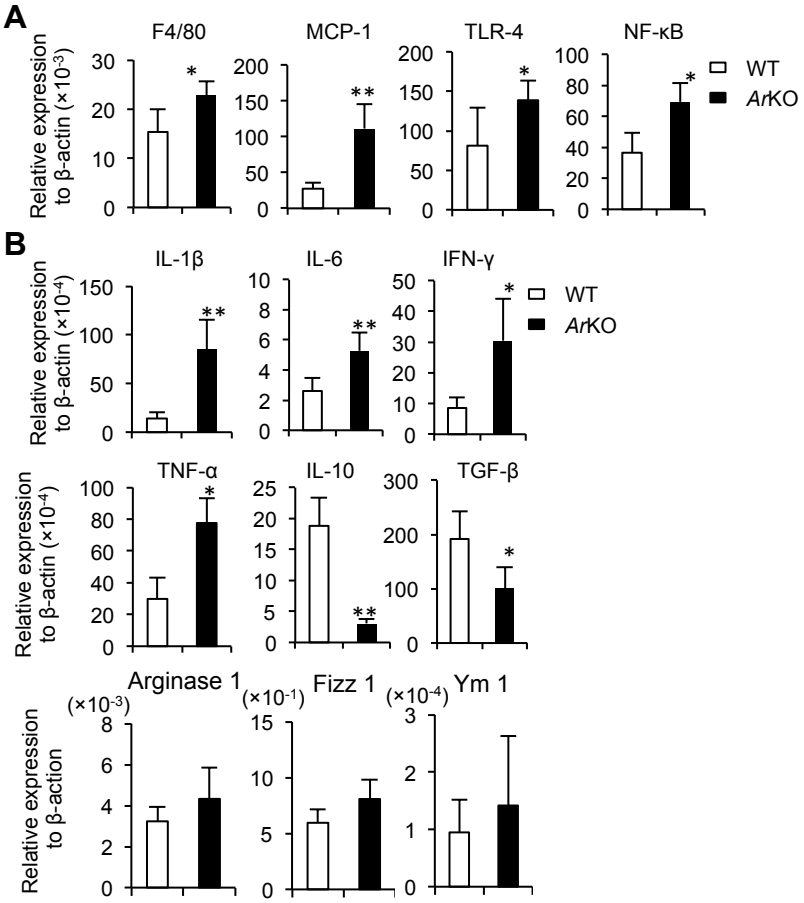
A
F4/80
MCP-1
TLR-4
NF-κB
Relative expression to β-actin (×10-3)
WT
ArKO
B
IL-1β
IL-6
IFN-γ
Relative expression to β-actin (×10-4)
TNF-α
IL-10
TGF-β
Arginase 1
Fizz 1
Ym 1
(×10-3)
(×10-1)
(×10-4)
Relative expression to β-action

Figure 4

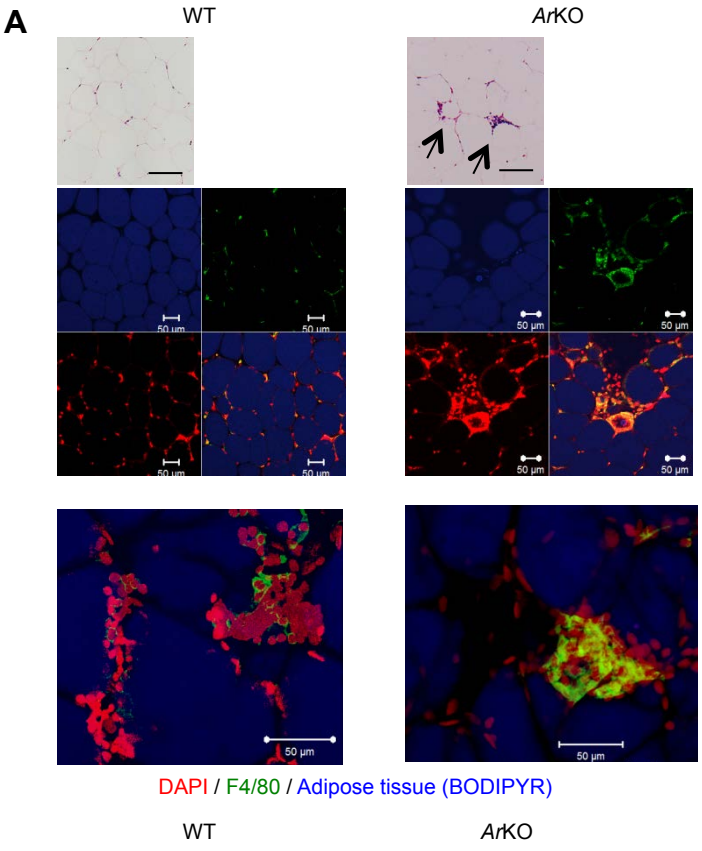
A
WT
ArKO
50 μm
DAPI / F4/80 / Adipose tissue (BODIPYR)
WT
ArKO
B
Gated on F4/80+
CCR2 (M1)
CD206 (M2)
WT
ArKO
27.5
35.9
52.5
21.6
CCR2 (M1)
CD206 (M2)
Positive cells (%)
60
40
20
0
**
*
WT
ArKO

Figure 5

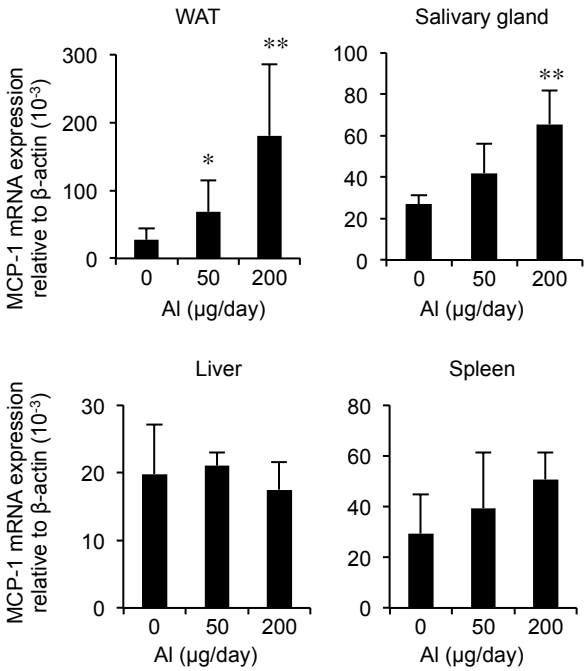
WAT
Salivary gland
Liver
Spleen
MCP-1 mRNA expression relative to β-actin (10-3)
Al (μg/day)
0
50
200
*
**

Figure 6

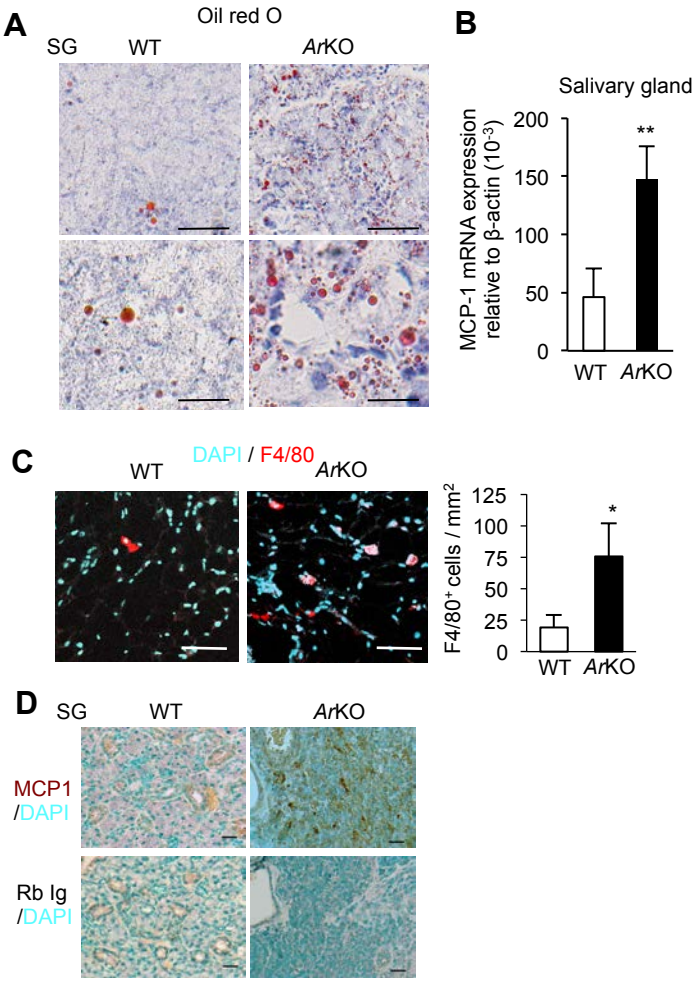
A
Oil red O
SG
WT
ArKO
B
Salivary gland
MCP-1 mRNA expression relative to β-actin (10-3)
200
150
100
50
0
**
WT
ArKO
C
DAPI / F4/80
WT
ArKO
F4/80+ cells / mm2
125
100
75
50
25
0
*
WT
ArKO
D
SG
WT
ArKO
MCP1 /DAPI
Rb Ig /DAPI

Figure 7

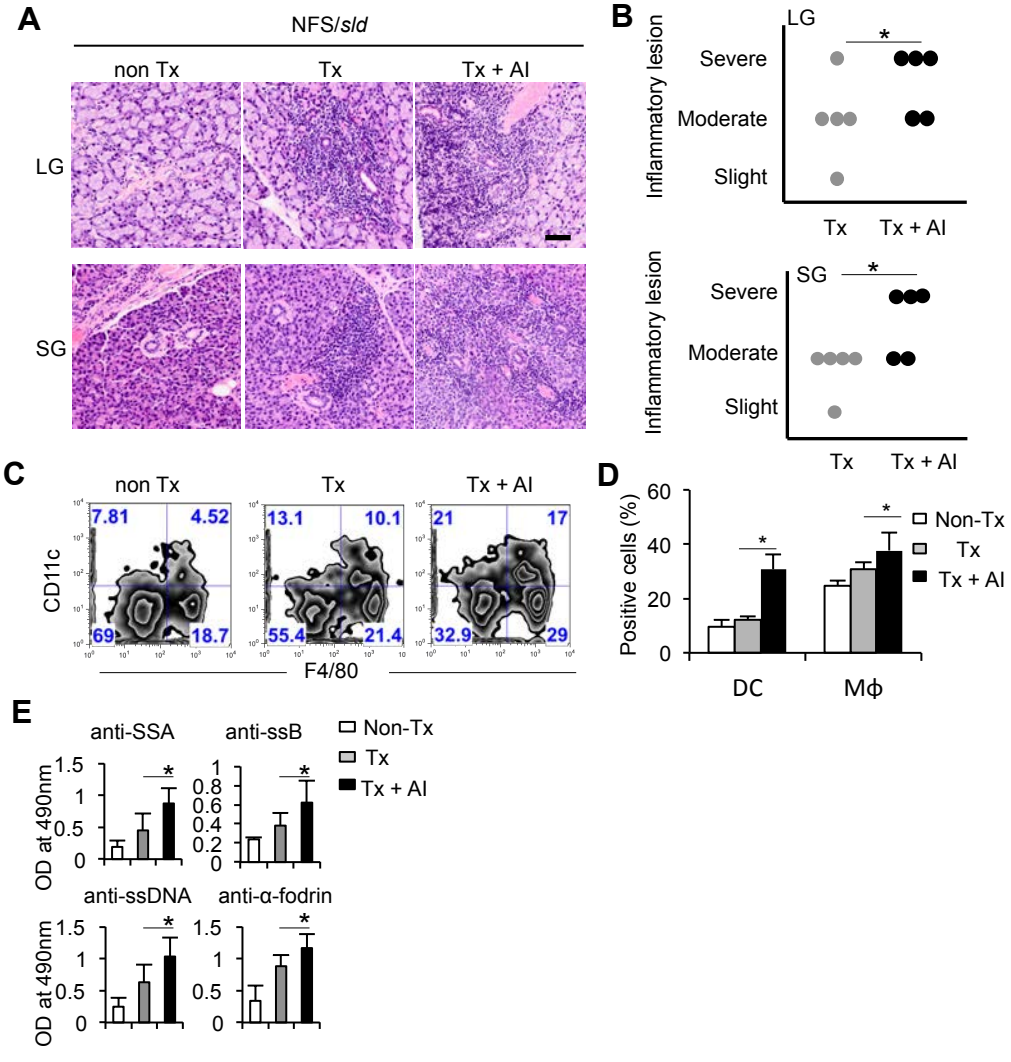
A
NFS/sld
non Tx
Tx
Tx + AI
LG
SG
B
LG
Severe
Moderate
Slight
Inflammatory lesion
Tx
Tx + AI
SG
C
non Tx
Tx
Tx + AI
7.81
4.52
69
18.7
13.1
10.1
55.4
21.4
21
17
32.9
29
CD11c
F4/80
D
Positive cells (%)
Non-Tx
Tx
Tx + AI
DC
Mϕ
E
anti-SSA
anti-ssB
anti-ssDNA
anti-α-fodrin
OD at 490nm